

## Lattice Boltzmann Method for Heterogeneous Multi-Class Traffic Flow

Romain Noël , Laurent Navarro & Guy Courbebaisse

To cite this article: Romain Noël , Laurent Navarro & Guy Courbebaisse (2020): Lattice Boltzmann Method for Heterogeneous Multi-Class Traffic Flow, Journal of Computational and Theoretical Transport, DOI: [10.1080/23324309.2020.1828468](https://doi.org/10.1080/23324309.2020.1828468)

To link to this article: <https://doi.org/10.1080/23324309.2020.1828468>



© 2020 The Author(s). Published with license by Taylor & Francis Group, LLC



Published online: 23 Nov 2020.



Submit your article to this journal [↗](#)



Article views: 37



View related articles [↗](#)



View Crossmark data [↗](#)

# Lattice Boltzmann Method for Heterogeneous Multi-Class Traffic Flow

Romain Noël<sup>a</sup> , Laurent Navarro<sup>a</sup> , and Guy Courbebaisse<sup>b</sup> 

<sup>a</sup>Mines Saint-Étienne, Univ. Lyon, Univ. Jean Monnet, INSERM, Saint-Étienne, France; <sup>b</sup>Univ. Lyon, INSA-Lyon, Université Claude Bernard Lyon 1, UJM Saint-Étienne, CNRS, INSERM, CREATIS UMR 5220, Lyon, France

## ABSTRACT

Traffic modeling often keeps the mesoscopic scale in the theoretical sphere because of the integro-differential nature of its equations. In the present work, it is suggested to use the lattice Boltzmann method to overcome these difficulties while benefiting the strong theoretical foundation of the method. An alternative version of the lattice Boltzmann method for multi-class and heterogeneity in traffic flow is elaborated in this paper. Its ability to reproduce the fundamental diagram is proved, for both single-class and multi-class flows. This allows easily simulating complex and realistic cases of mixture of multi-class traffic flow. These simulations are able to capture jamming in various traffic situations such as road merging, reduction of the number of lanes or change of speed limits.



## KEYWORDS

Heterogeneous traffic flow; multi-class flow; Boltzmann-like equations; lattice Boltzmann method

## 1. Introduction

Since the end of the twentieth century, with the increase of personal car and road jam, traffic modeling has become a topic in the center of economic, ecological, and social considerations. In this context, constructors and road operators look forward to having a better understanding and anticipation of traffic flows, in order to recommend the optimal practical solutions.

In this perspective, the models should handle the heterogeneous characteristics of the traffic flow. One of its major heterogeneity is its composition by multiple classes (or categories) of vehicles. Road operators and car drivers agree on the important role of lorries. Due to their longer dimensions and heavier weight, they are incriminated for faster deterioration of the structures, densification of traffic situations, slowing of flows and faster creation of traffic jams for a longer time.

**CONTACT** Romain Noël  [romainoel@free.fr](mailto:romainoel@free.fr)  Mines Saint-Étienne, Univ. Lyon, Univ. Jean Monnet, INSERM, Saint-Étienne, France.

© 2020 The Author(s). Published with license by Taylor & Francis Group, LLC

This is an Open Access article distributed under the terms of the Creative Commons Attribution-NonCommercial-NoDerivatives License (<http://creativecommons.org/licenses/by-nc-nd/4.0/>), which permits non-commercial re-use, distribution, and reproduction in any medium, provided the original work is properly cited, and is not altered, transformed, or built upon in any way.

Models have to be able to capture various nonlinear phenomena, such as those responsible for the growth of traffic jams. Commonly traffic models are classified in three groups: microscopic, mesoscopic and macroscopic. First, microscopic models describe the behavior of each driver individually. They allow the interaction between two vehicles to be studied finely and simulated to investigate its impact on traffic flows. This level of detail allows including the psychological aspect of the drivers. At the microscopic scale, the lane-changing and the overtaking questions are crucial (Gazis, Herman, and Rothery 1961; Gipps 1981; Kerner 1999). These models are very suited to simulate the evolution of traffic inside cities' streets but also what could be the new traffic behaviors with intelligent or unmanned vehicles (Chen et al. 2010; Delis, Nikolos, and Papageorgiou 2018; Pourabdollah et al. 2017; Talebpour and Mahmassani 2016; Wu et al. 2017). The most widely used method in these approaches is the cellular automaton (Chopard, Luthi, and Queloiz 1996; Nagel and Schreckenberg 1992; Nagel et al. 1998; Schadschneider and Schreckenberg 1993) and the car-following theory (Newell 1993, 2002; Pipes 1967). The main counterpart of the microscopic scale is the numerical resources needed to simulate large areas or numerous vehicles. This need is due to the number of differential equations necessary to solve for car-following methods, and the repeat of simulations in order to improve signal-to-noise ratio with the cellular automaton.

At the opposite of these approaches, the macroscopic models have high computational efficiency. This efficiency is mainly obtained thanks to the reduced number of macroscopic variables describing the traffic flow and the nature of the partial differential equations ruling these variables (Payne 1971). Such models results of the mixture of the empirical behavior like the fundamental diagram and hydrodynamics equations. One could cite the famous LWR model Lighthill and Whitham (1955) and Richards (1956). These are appropriate models for long roads where the position and velocity of each vehicle are not at stake nor significant.

Mesoscopic models use a statistical description to recover the macroscopic equations with a finer level of detail. These approaches adapt the kinetic theory of ideal gases to traffic situations (Prigogine and Herman 1971). They are based on Boltzmann-like equations, therefore they rely on the microscopic interactions, which give "physical" explanation and foundations to the resulting behaviors. Mesoscopic and macroscopic traffic flow models can be derived rigorously from microscopic dynamics (Helbing et al. 2002; Treiber and Kesting 2013). On the one hand, the main mesoscopic variable is the distribution function, reducing the numbers of variables and the computation time. On the other hand, the price of having fine details and numerical efficiency is the necessity to work in functional spaces and the complexity of the Boltzmann-like equations and their solutions.

The multi-class effects are challenging and have been studied at all scales. At the macroscopic scale, various multi-class works have been proposed (Jiang and Wu 2004; Logghe and Immers 2008). At a microscopic scale, approaches using cellular automaton (Lan and Chang 2005) or car-following (Hidas 2002; Peeta, Zhang, and Zhou 2005) but also mixtures of (cooperative) adaptive cruise control or intelligent driver model and human-driven vehicles (Chen et al. 2010; Delis, Nikolos, and Papageorgiou 2018; Kesting, Treiber, and Helbing 2010; Pourabdollah et al. 2017; Talebpour and Mahmassani 2016; Wu et al. 2017) have been developed. The mesoscopic scale has also been the object of very detailed works for multi-class traffic flow, where the interactions between classes are viewed from statistics (Chanut 2005; Hoogendoorn and Bovy 2000, 2001; Shvetsov and Helbing 1999; Treiber and Kesting 2013).

The Lattice Boltzmann Method (LBM) is born after the statistical averaging for lattice gas cellular automata, in order to have meaningful results when simple simulations are subjected to numerical noise. Yet, the LBM also has a strong theoretical base lying on the Boltzmann equation He and Luo (1997). Thus, it seems to be a natural framework to build numerical schemes for mesoscopic models. However, few examples of LBM for traffic flow are currently available.

In the present work, a statistical description of continuous kinetic model is introduced in detail, before discussing the effects of multi-class heterogeneity on continuum models. Then the construction of the lattice Boltzmann method and the formulations associated, for both the single class and heterogeneous multi-class frameworks are proposed. It is followed by numerical simulations in order to validate the suggested model. Finally, discussions and conclusions are given in the last section.

## 2. Statistical description

### 2.1. Continuous kinetic models

To build a continuous mesoscopic and kinetic model, the density of vehicles  $\rho$  has to be studied at a spatial position  $x$  along a highway, at a time  $t$ . Obviously, on multi-lane roads, several vehicles can be at the same time and position with a different velocity. This remark is also true, with single-lane roads, since the Representative Elementary Volume (REV) used for the mesoscopic scale is such that it contains many vehicles. Naturally, this leads to introduce  $f(x, \xi, t)$  the distribution of vehicles with the velocity  $\xi$ . By working in the velocity space, the density  $\rho$ , average speed  $v$ , and flow  $q$  are given by:

$$\rho(x, t) = \int f(x, \xi, t) d\xi \quad (1)$$

$$q(x, t) = \rho(x, t)v(x, t) = \int \xi f(x, \xi, t) d\xi. \quad (2)$$

To describe the evolution of any distribution of particles, Boltzmann suggested using the sum of a transport term with interactions between these particles. It is quite reasonable to consider vehicles as particles interacting. Following this idea, the Boltzmann equation seems perfectly adapted to vehicle transport problems linked to traffic flow. Thus, Prigogine and Andrews (1960) and Prigogine and Herman (1971), suggested describing the evolution with no “external forces” and by decomposing the collision-interaction operator into two terms. The *Prigogine-Boltzmann equation* for traffic flow is

$$\left( \frac{\partial}{\partial t} + \xi \frac{\partial}{\partial x} \right) f = \Omega(f, f) = \left( \frac{\partial f}{\partial t} \right)_{rel} + \left( \frac{\partial f}{\partial t} \right)_{int} \quad (3)$$

where the left-hand side member is the transport term,  $\Omega$  is the collision-interaction operator,  $\left( \frac{\partial f}{\partial t} \right)_{rel}$  and  $\left( \frac{\partial f}{\partial t} \right)_{int}$  are respectively the relaxation term and the interaction term.

The relaxation term is assuming that drivers will reach a certain speed called desired velocity. This desired velocity for all drivers is described by a distribution function  $f^d$ , and it is reached after a certain time  $\tau$  called the relaxation time. Therefore, the relaxation term can be expressed as:

$$\left( \frac{\partial f}{\partial t} \right)_{rel} = - \frac{f(x, \xi, t) - f^d(x, \xi, t)}{\tau}. \quad (4)$$

The interaction term renders the following overtaking process. When a fast incoming vehicle attains a slower one, the slow one is not affected. If the fast one cannot overtake it, the fast driver has to slow down in a short period. So, the interaction term not only encompasses overtaking maneuvers but also braking maneuvers when the overtaking is not possible. The interaction term can be given by:

$$\left( \frac{\partial f}{\partial t} \right)_{int} = (1-p)f(x, \xi, t) \int (\xi' - \xi) f(x, \xi', t) d\xi' \quad (5)$$

where  $p$  denotes the average probability to overtake slow vehicles *id est* the slowing down event has the probability  $(1-p)$ .

This model is criticized by some authors Munjal and Pahl (1969). Paveri-Fontana highlighted some problems with this model when  $\tau$  and  $p$  are constant. He also suggests a close enhanced model Paveri-Fontana (1975). Moreover, he shows that Prigogine-Boltzmann equation and the

Paveri-Fontana improved Boltzmann equation yield the same macroscopic equation up to the second order.

Thus, as a first approach the Prigogine-Boltzmann equation is a simpler and a good description of the traffic flow if  $\tau$  and  $p$  are linked to the vehicle density. A common relationship between the parameter  $p$  and the density  $\rho$  is  $\gamma = \tau\rho(1-p)$ , where  $\gamma$  is a constant. To have a model closer to the conventional lattice Boltzmann method, the Prigogine-Boltzmann equation can be rewritten

$$\left(\frac{\partial}{\partial t} + \xi \frac{\partial}{\partial x}\right) f(x, \xi, t) = \frac{f^{(0)} - f}{\tau'} \quad (6)$$

with

$$f^{(0)} = \frac{\tau'}{\tau} f^d + \left(1 - \frac{\tau'}{\tau}\right) \rho(\xi - v) \quad \tau' = \frac{\tau}{1 + \gamma}.$$

In the following, the distribution  $f^{(0)}$  is called equilibrium distribution function.

Some authors continue this path to create generic kinetic traffic models adapted to many situations (Helbing 2001; Treiber and Kesting 2013). Despite the discussions about the validity of their assumptions (specially about the vehicular chaos), the continuous kinetic models seem to be good tools to deal with traffic flows.

## 2.2. Continuum kinetic multi-class traffic approach

Some authors Costeseque and Duret (2015) and Hoogendoorn and Bovy (2000) constructed continuum kinetic models for multi-class flows, through numerous inter-class interactions. However, others Bagnerini and Rasle (2003) and Chanut (2005) remind that the use of multi-class distribution is easier.

In this work, an alternative and simpler formulation is used. Indeed, guided by the intuition that each driver interacts on average in the same manner with all the other vehicles, independently of the class of the other vehicles, the construction of the equilibrium distribution for each class should be the function of the global density over the class and the local density of its own class to respect the continuity equation.

Let us denote with the subscript  $c$  one class of vehicle out of  $N_c$  the number of classes. Thus, the mesoscopic multi-class Boltzmann-like equations are

$$\left(\frac{\partial}{\partial t} + \xi \frac{\partial}{\partial x}\right) f_c(x, \xi, t) = \frac{f_c^{(0)}(\rho, \rho_c) - f_c}{\tau'_c} \quad (7)$$

$$\rho_c(x, t) = \int f_c(x, \xi, t) d\xi \quad (8)$$

$$q_c(x, t) = \rho_c v_c(x, t) = \int \xi f_c(x, \xi, t) d\xi \quad (9)$$

$$\rho = \sum_{c=1}^{N_c} \rho_c \quad q = \rho v = \sum_{c=1}^{N_c} q_c. \quad (10)$$

To be more accurate, density  $\rho$  and  $\rho_c$  considered here should be interpreted as non-dimensional density or equivalently as occupation rates. More precisely, let us consider the case of two classes, the first one made of vehicles of length  $L_1$  and the second one of length  $L_2$ . If the length of the REV is  $D_x$ , therefore the maximum number of vehicles from the first class at the position  $x$  is denoted  $\bar{\rho}_1(x)$  and has the maximum value of  $D_x/L_1$ . This value is reached when there is no free space between vehicles, which leads to the definition of  $\rho_c$  as the occupation rate. Therefore for any class, the relationship between  $\rho$  and  $\bar{\rho}$  is

$$\bar{\rho}_c(x) = \frac{D_x}{L_c} \rho_c(x). \quad (11)$$

Moreover, the global density can only be expressed in terms of vehicles number equivalent to vehicles of one class. In the previous example, the number of vehicles from the second class equivalent to the ones of the first class is  $\bar{\rho}_{2/1} = \bar{\rho}_2 L_2 / L_1$ . And so, if  $\bar{\rho}_{tot/1}$  is the total number of vehicles equivalent to those of the first class, this number is given by

$$\bar{\rho}_{tot/1} = \sum_{c=1}^{N_c} \rho_c \frac{L_c}{L_1} = \rho \frac{D_x}{L_1} \quad (12)$$

which is more convenient to compute with rate occupations (see [Equation \(10\)](#)).

The major drawback with kinetic models (single or multi-class) is the integro-differential nature of their equations. This fact, combined with the lack of physical properties, is responsible for absence of analytical solutions. This is why numerical methods are for now necessary.

### 3. Lattice Boltzmann method

#### 3.1. Lattice Boltzmann model for heterogeneous traffic flows

The LBM is a numerical method to solve a discretization of the continuous Boltzmann equation. This discretization is performed on all three space, time, and velocity space. Time discretization gives an explicit schema. The velocity space discretization is often denoted  $DnQm$  where  $n$  specifies the physical dimension of the problem and  $m$  is the number of points used to condense the velocity space. The denomination lattice is linked to the

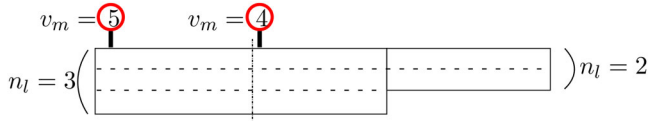


**Figure 1.** Schematic of a road with changing of the speed limit and number of lanes.

regular spatial discretization and the  $DnQm$  schema used to connect the spatial points; to coincide with the velocities Succi (2001).

Commonly in the LBM approach, the assumption of a collision-interaction operator composed only of a relaxation term is made. This assumption is named Bhatnagar, Gross and Krook (BGK) in reference to its authors Bhatnagar, Gross, and Krook (1954). Thus, under the BGK approximation the Lattice Boltzmann Equation (LBE) reads Chopard et al. (2002) and Wolf-Gladrow (2000)

$$f_i(x + e_i \delta_t, t + \delta_t) = f_i(x, t) + \frac{1}{\tau} (f_i^{(0)} - f_i) \quad (13)$$

where  $f_i$  is the distribution evaluated in  $e_i$  the discrete velocities (associate to the velocity space);  $\delta_t$  is the time step, therefore the space or lattice step is given by  $\delta_x / \delta_t = e$  and  $e_i = i \delta_x / \delta_t$ .

For the numerical resolution, the LBE is divided in two steps. The first step is the collision-interaction step defined by the equation

$$f_i(x, t + \delta_t) = f_i(x, t) + \frac{1}{\tau} (f_i^{(0)} - f_i). \quad (14)$$

This is usually followed by the streaming step defined by:

$$f_i(x + e_i \delta_t, t + \delta_t) = f_i(x, t + \delta_t). \quad (15)$$

Nevertheless, the last equation comes from fluid dynamics and must be adapted to take into account possible lane number changes (see Figure 1). Therefore, to face these possibilities, it is suggested to turn the Equation (15) into:

$$f_i(x + e_i \delta_t, t + \delta_t) = f_i(x, t + \delta_t) \frac{n_l(x)}{n_l(x + e_i \delta_t)} \quad (16)$$

with  $n_l$  the number of lanes for a given spatial point.

The macroscopic variables are recovered by using the classic following summations:

$$\rho(x, t) = \sum_{i=0}^{m-1} f_i(x, t) \quad (17)$$

$$q(x, t) = \rho v(x, t) = \sum_{i=0}^{m-1} e_i f_i(x, t). \quad (18)$$



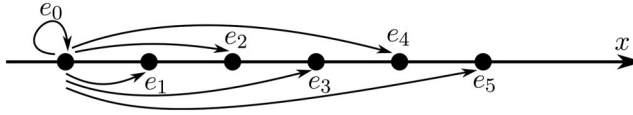


**Figure 2.** Schematic of an asymmetric  $D1Q6$  network.

The LBM in its classical form can solve various problems related to transport of particles, under certain conditions like compressible or viscous flows. The equilibrium distribution function has to be in adequacy with the physical phenomena. This distribution function is, in the Euler conservation case, uniquely found through the application of mathematical theorem Cercignani (1988) and physical conservation laws.

When applying the LBM for road traffic (Meng et al. 2008; Shi et al. 2016), the lack of conservation laws makes the appreciation of the equilibrium distribution function harder. As some authors suggest Meng et al. (2008) a work-around by constructing it from the observable data could be adopted. The other noticeable difference with the LBM applied to traffic problems is the velocity space. It is  $\mathbb{R}^n$  (symmetric) for fluids or gases but it becomes  $\mathbb{R}^+$  (asymmetric) with roads since the dimension of roads is one and vehicles almost never use reverse gear for something else than to park. Therefore it is suggested to use a  $D1q6$  schema (see Figure 2), or more.

Previous studies Meng et al. (2008) suggest choosing an equilibrium distribution function that offers interesting capacity to model empirical phenomena. Here, a completeness of this empirical model to deal with heterogeneity is introduced. It allows to define the equilibrium distribution function with

$$f_i^{(0)} = \begin{cases} \frac{\rho(x)}{1 + \sum_{i=1}^{v_m} e_i^2 \exp\left(-\frac{e_i^2 \tilde{\rho}(x)}{1 - \tilde{\rho}(x)}\right)} & \text{for } i = 0 \\ \frac{e_i^2 \exp\left(-\frac{e_i^2 \tilde{\rho}(x)}{1 - \tilde{\rho}(x)}\right) \rho(x)}{1 + \sum_{i=1}^{v_m} e_i^2 \exp\left(-\frac{e_i^2 \tilde{\rho}(x)}{1 - \tilde{\rho}(x)}\right)} & \forall i \in [[1, v_m]] \\ 0 & \forall i \in [[v_m + 1, m - 1]] \end{cases} \quad (19)$$

$$\tilde{\rho}(x) = \frac{\sum_{i=0}^{v_m} \rho(x + e_i)}{v_m + 1} \quad (20)$$

where  $v_m$  is the maximum speed of vehicles (it can be the speed limit, like on Figure 1, or higher values, if one wants to capture over-speeding) and  $\tilde{\rho}$  is the most important parameter. The latter can be seen as the reachable

forward occupation rate. In other words, it is the density, that the drivers feel in front of them, in which they will have to navigate. Obviously, the maximum speed of vehicles  $v_m$  is an integer lower than or equal to the maximum speed used to model the system  $m - 1$ . This also means that the variations of  $v_m$  along the road can only be a multiple of the lattice step  $\delta_x/\delta_t = e$ .

This equilibrium distribution function expressed the fact that drivers under a constant relaxation time, change their desired speed with the variation of the forward reachable occupation rate. It is a manner to express that they are adapting their speed with the traffic.

This model has to be completed by “virtual boundary condition” to prevent having density higher than one when too many vehicles from different cells want to reach the same cell. Naturally, the vehicles from the further cells have to slow down quickly.

$$B_v(f_i(x)) = \begin{cases} f_i^*(x - e_i \delta_t) = \begin{cases} 0 & \text{if } \rho_{test} - \sum_{j=i+1}^m f_j(x - e_j \delta_t) \frac{n_l(x - e_j \delta_t)}{n_l(x)} > 1 \\ f_i(x - e_i \delta_t) & \text{else} \end{cases} \\ f_{i-1}^*(x - e_i \delta_t) = \begin{cases} f_i(x - e_i \delta_t) + f_{i-1}(x - e_i \delta_t) & \text{if } \rho_{test} - \sum_{j=i+1}^m f_j(x - e_j \delta_t) \frac{n_l(x - e_j \delta_t)}{n_l(x)} > 1 \\ f_{i-1}(x - e_i \delta_t) & \text{else} \end{cases} \end{cases} \quad (21)$$

$$\rho_{test}(x) = \sum_{i=0}^m f_i(x - e_i \delta_t) \frac{n_l(x - e_i \delta_t)}{n_l(x)}. \quad (22)$$

A virtual boundary condition inspired by Meng et al. (2008), can be expressed through the function  $B_v$  (see Equation (21)), in which the quantity  $\rho_{test}$  (see Equation (22)) represents the density that would happen if all the drivers could stream as they wish, i.e., if the density could be greater than one and so that car crash could happen.

To avoid any confusion, since in the definition of  $B_v$  the comparison is made with 1, the definition of  $\rho$  or  $\rho_{test}$  used here is the occupation rate varying from 0 to 1.

Thus it is suggested to rewrite the streaming step that takes into account the virtual boundaries:

$$f_i(x + e_i \delta_t, t + \delta_t) = B_v(f_i(x, t + \delta_t)). \quad (23)$$

### 3.2. Lattice Boltzmann model for multi-class traffic

Strengthened by the successful results of the LBM to model the Navier-Stokes equations, researchers quickly tackled more complex problems like mixture of fluids. A noticeable work has been done in the case of

immiscible mixture (Shan and Chen 1993). At the same time, some pioneers initiated the work on miscible fluids (Holme and Rothman 1992), improved some years after by adding thermodynamics equations (Inamuro et al. 2002).

When it comes to traffic, despite heavy machinery vehicles tend to form a continuous lane on highways, the second lane is most of the time full of personal car. So, the hypothesis of immiscibility seems not to be the most relevant in a first approach. Even if, publications deal with the use of cellular automata for multi-class traffic flows (Ez-Zahraouy, Jetto, and Benyoussef 2004); the use of the lattice Boltzmann method to solve heterogeneous multi-class traffics has never been studied.

To take into account the necessity for the equilibrium density function to depend on the global density and the class density, and since the variable  $\tilde{\rho}$  can be understood as the density felt forward drivers; it seems natural in a first approach that the global density depends only on  $\tilde{\rho}$ . Thus, the macroscopic variable related to the Equation (10) can be written as

$$\rho_c = \sum_{i=0}^{m-1} f_{c,i}(x, t) \quad q_c = \sum_{i=0}^{m-1} e_i f_{c,i}(x, t) \quad (24)$$

$$\rho = \sum_{c=1}^{N_c} \rho_c = \sum_{i=0}^{m-1} \sum_{c=1}^{N_c} f_{c,i}(x, t) \quad (25)$$

$$q = \sum_{c=1}^{N_c} q_c = \sum_{c=1}^{N_c} \sum_{i=0}^{m-1} e_i f_{c,i}(x, t). \quad (26)$$

Then, the respect of conservation equations leads to a new formulation of the equilibrium density function:

$$f_{c,i}^{(0)} = \begin{cases} \frac{\rho_c(x)}{1 + \sum_{i=1}^{v_{m,c}} e_i^2 \exp\left(-\frac{e_i^2 \tilde{\rho}_c(x)}{1 - \tilde{\rho}_c(x)}\right)} & \text{for } i = 0 \\ \frac{e_i^2 \exp\left(-\frac{e_i^2 \tilde{\rho}_c(x)}{1 - \tilde{\rho}_c(x)}\right) \rho_c(x)}{1 + \sum_{i=1}^{v_{m,c}} e_i^2 \exp\left(-\frac{e_i^2 \tilde{\rho}_c(x)}{1 - \tilde{\rho}_c(x)}\right)} & \forall i \in [[1, v_{c,m}]] \\ 0 & \forall i \in [[v_{c,m} + 1, m]] \end{cases} \quad (27)$$

$$\tilde{\rho}_c(x) = \frac{\sum_{i=0}^{v_{m,c}} \rho(x + e_i)}{v_{m,c} + 1} \quad (28)$$

where  $v_{m,c}$  is the maximum speed of the class  $c$  vehicles, and  $\tilde{\rho}_c$  is the reachable forward occupation rate for the class  $c$ .

The virtual boundary conditions also have to follow the same logic. One should note that since the  $B_v$  function affects the values of the distribution at a point backward from a given point where variables are evaluated, its algorithmic application should be backward recursive. The variable  $\rho_{test}$  has to be the reflection of the global density, while the modifications over density has to be accomplished per class. Therefore, the virtual boundaries can be expressed by:

$$B_v(f_i(x)) = \begin{cases} f_{i,c}^*(x-e_i\delta_t) & = \begin{cases} 0 & \text{if } \rho_{test} - \sum_{\substack{i+1 \leq j \leq m \\ 0 \leq c \leq N_c}} f_{j,c}(x-e_j\delta_t) \frac{n_l(x-e_j\delta_t)}{n_l(x)} > 1 \\ f_{i,c}(x-e_i\delta_t) & \text{else} \end{cases} \\ f_{i-1,c}^*(x-e_i\delta_t) & = \begin{cases} f_{i,c}(x-e_i\delta_t) + f_{i-1,c}(x-e_i\delta_t) & \text{if } \rho_{test} - \sum_{\substack{i+1 \leq j \leq m \\ 0 \leq c \leq N_c}} f_{j,c}(x-e_j\delta_t) \frac{n_l(x-e_j\delta_t)}{n_l(x)} > 1 \\ f_{i-1,c}(x-e_i\delta_t) & \text{else} \end{cases} \end{cases} \quad (29)$$

$$\rho_{test}(x) = \sum_{i=0}^m \sum_{c=0}^{N_c} f_{i,c}(x-e_i\delta_t) \frac{n_l(x-e_i\delta_t)}{n_l(x)}. \quad (30)$$

#### 4. Validation through numerical simulations

In all the following simulations, a space step of 5.5 meters and a time step of 1 second are taken. This leads to a speed step of almost 20 kilometers per hour. Moreover, a  $D1Q6$  schema is used, consequently the maximum speed is close to 100 kilometers per hour. However, for the sake of generality, the following results will be presented in their non-dimensional form, i.e., expressed in space or time step units.

All the following simulations are obtained with a relaxation frequency of 0.9, with the exception of the simulations linked to [Figure 5](#) where the value of the relaxation time is varying. The presented model is here confronted with different simulations: fundamental diagrams, speed limits and number of lane changes, road merging, and variation of truck concentration.

##### 4.1. Fundamental diagrams

To evaluate the behavior of the suggested model, the study of density-flow fundamental diagram is performed. It allows estimating the relationship between the flow and the density (Kerner, Klenov, and Wolf 2002; Ngoduy 2011). The study of a ring road, of 1000 cell length, simulated for different average density is done. Each simulation starts with density spatially varying around the average density by following a random noise of 10%. The road has a speed restriction of 5 cells per unit of time (see [Figure 3](#)).

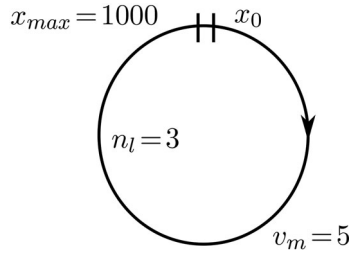


**Figure 3.** Schematic of a ring road.

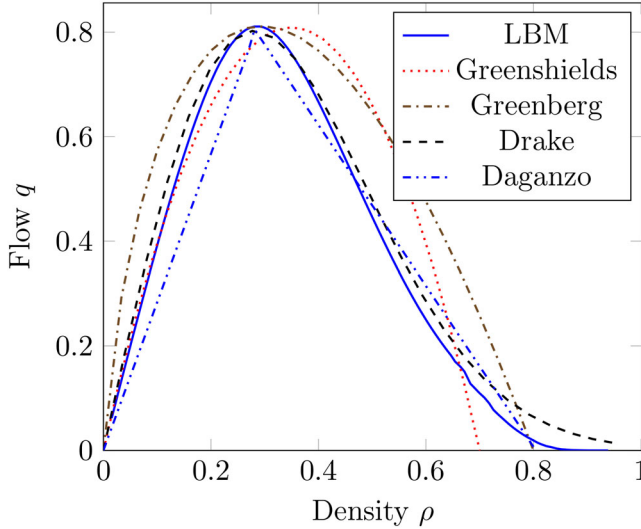


**Figure 4.** Fundamental diagram of some macroscopic models.

The relaxation time is set to 0.9. After 2000 time steps, the averaging over time and space is made to obtain the [Figure 4](#). The resulting curve is compared to usual macroscopic models such as the Greenshields (1935), Greenberg (1959), Drake, Schofer, and May (1967), or Daganzo (1997) models.

[Figure 4](#) shows the ability of the LBM to simulate the various traffic situations with good accuracy. The results are very close to those described by the Drake model (Drake, Schofer, and May 1967).

Moreover, the effect of the relaxation time on the fundamental diagram is major. This effect is represented on the [Figure 5](#). The relaxation time interval in which the numerical schema remains stable is directly linked to the equilibrium distribution function suggested. Moreover, the fact that its effect is only noticeable for congested-flow can be interpreted as the too slow ability of the drivers to change (or reach) their desire speed. In other words, they have a speed incompatible with the current density of traffic.

For values of the relaxation time higher than 1.20 and lower than 0.65, the numerical model becomes unstable for high density. This is due to the

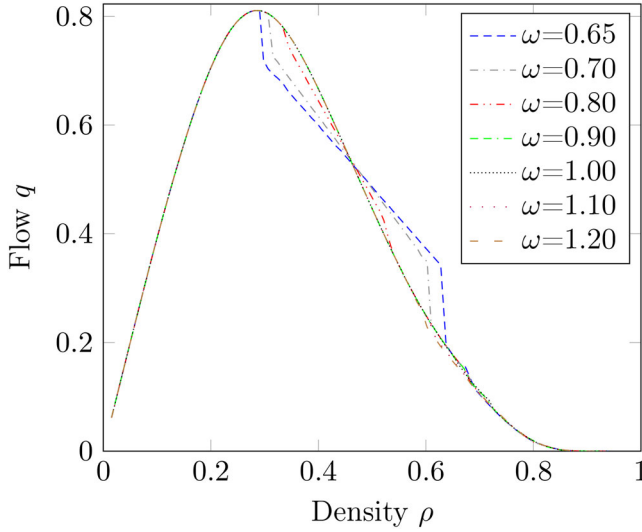


**Figure 5.** Flow-density relationship for different relaxation time.

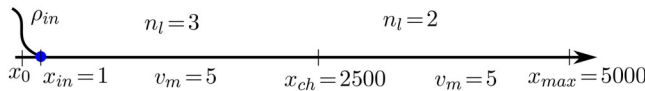


**Figure 6.** Schematic of a road with a number of lane change.

nature of the equilibrium distribution function, which is a compromise between the desired velocity and the current velocity. Therefore, a high relaxation time means drivers not breaking enough in case of slowing down, and a low relaxation time means drivers over accelerating in case of speeding up. Both the acceleration and breaking phenomenon are critical at high density since the start and stop occur with limited margins to maneuver in strong jam. In both high and low relaxation time, the maladjusted behaviors of the drivers lead to instabilities.

#### 4.2. Number of lane

To evaluate the effect of a change of lane number on traffic conditions; the study of a road of 5000 sites is proposed. It starts with three lanes and a constant density, while a reduction to two lanes is located at the site number 2500. The speed limit is set to 5 cells per unit of time, as shows [Figure 6](#).

[Figure 7](#) represents density evolution in time and space for a simulation with the entrance density of 0.10 (see [Table 1](#)). This situation leads to a density increase after the reduction of lanes, which remains in free-flow domain.

[Figure 8](#) has for incoming density 0.20 (see [Table 2](#)), which means that an increase of its density will lead to the congested-flow domain and might create

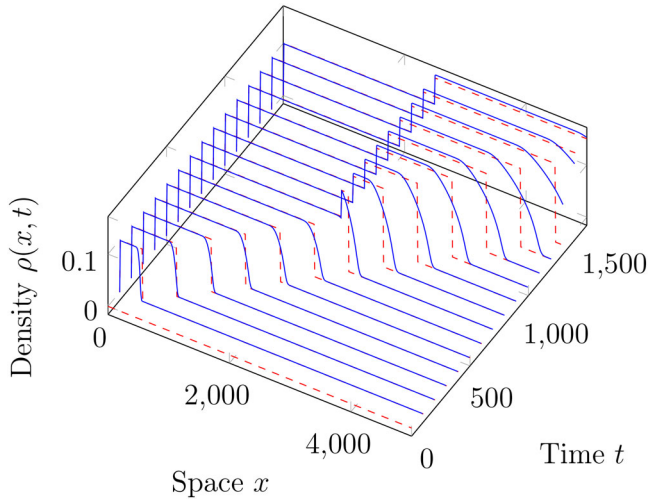


**Figure 7.** Density for reduction of lanes in free-flow conditions: simulation with LBM in solid blue and with triangular-Daganzo fundamental diagram for LWR method in dashed red.

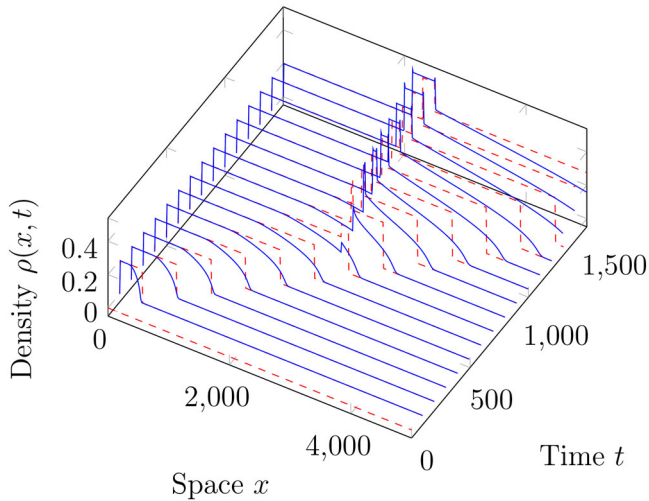


**Figure 8.** Density for a reduction of lanes in congested-flow traffic conditions: simulation with LBM in solid blue and with triangular-Daganzo fundamental diagram for LWR method in dashed red.

important interactions. On [Figure 8](#), the entrance in congested-flow domain leads to a slowing-down situation waving backward.

### 4.3. Speed limit change

The last external source of modification for traffic conditions studied in this section is the change of speed limit. The same length of the road than

**Table 1.** Parameters for the LBM modeling of a road containing a reduction of lanes in free-flow traffic conditions.

Parameters	Values	Space
$\rho_{in}$	0.10	$x_{in} = 1$
$n_l$	3	$\forall x \in [0, 2500]$
$v_m$	5	$\forall x \in [0, 2500]$
$n_l$	2	$\forall x \in [2500, 5000]$
$v_m$	5	$\forall x \in [2500, 5000]$

**Table 2.** Parameters for the LBM modeling of a road containing a reduction of lanes in congested-flow traffic conditions.

Parameters	Values	Space
$\rho_{in}$	0.20	$x_{in} = 1$
$n_l$	3	$\forall x \in [0, 2500]$
$v_m$	5	$\forall x \in [0, 2500]$
$n_l$	2	$\forall x \in [2500, 5000]$
$v_m$	5	$\forall x \in [2500, 5000]$

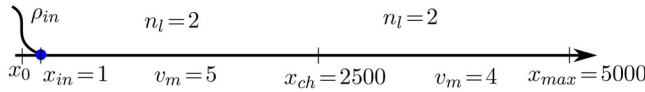


**Figure 9.** Schematic of a road with a change of speed limit.

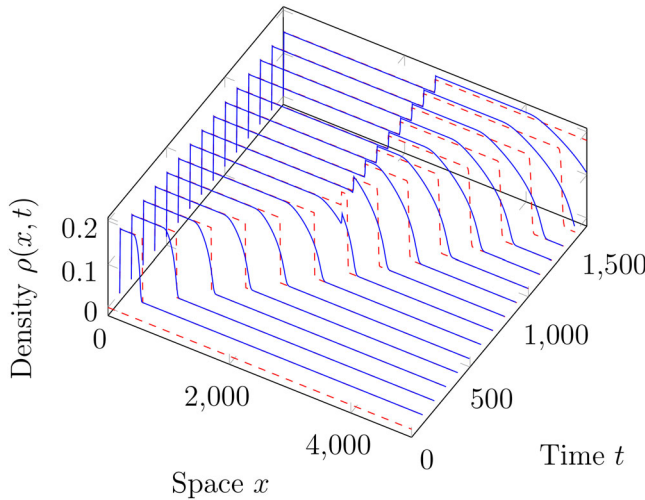


**Figure 10.** Modeling of a road containing a reduction of speed restriction under free-flow traffic conditions: simulation with LBM in solid blue and with triangular-Daganzo fundamental diagram for LWR method in dashed red.

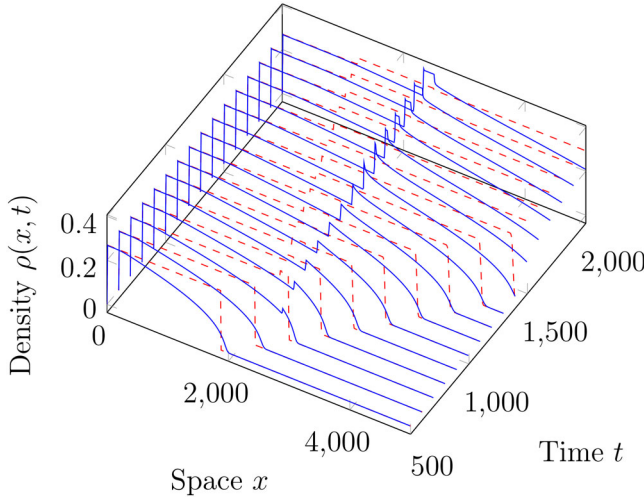
for the previous numerical investigations for a road of two lanes and the same relaxation frequency is used. As shown in Figure 9, a reduction of speed limits from 5 to 4 cells per unit of time is imposed on the site number 2500.

With the density of 0.15 at the entrance of the road (see Table 3), the speed limit reduction has the same effect as the reduction of the lane



**Table 3.** Parameters for the LBM modeling of a road containing a reduction of speed restriction under free-flow traffic conditions.

Parameters	Values	Space
$\rho_{in}$	0.15	$x_{in} = 1$
$n_l$	2	$\forall x \in [0, 2500]$
$v_m$	5	$\forall x \in [0, 2500]$
$n_l$	2	$\forall x \in [2500, 5000]$
$v_m$	4	$\forall x \in [2500, 5000]$

**Figure 11.** Modeling of a road containing a reduction of speed restriction under congested-flow traffic conditions: simulation with LBM in solid blue and with triangular-Daganzo fundamental diagram for LWR method in dashed red.

number: an increase in the density forward to the change. The [Figure 10](#) represents this situation with the increased density still in free-flow domain.

For [Figure 11](#), the entrance density set at 0.26 leads (see [Table 4](#)), after the reduction of speed limits, to a congested flow. It corresponds to the same consequences as the previous congested cases, i.e., a slowing down flow.

One can notice a difference between the results of the LBM and LWR methods on [Figure 11](#). The backward slowing down wave is starting earlier and is less dense than the one generated by the LBM. This can be largely explained by the differences in the fundamental diagrams between triangular-Daganzo and the LBM models. And this is emphasized by the fact that the reduction of speed restriction under congested-flow simulated involves the upper part of the fundamental diagram where the two diagrams are the most different. Despite this difference, the same phenomena of slowing down wave propagating backward from the reduction of speed restriction is clearly visible.

**Table 4.** Parameters for the LBM modeling of a road containing a reduction of speed restriction under congested-flow traffic conditions.

Parameters	Values	Space
$\rho_{in}$	0.26	$x_{in} = 1$
$n_l$	2	$\forall x \in [0, 2500]$
$v_m$	5	$\forall x \in [0, 2500]$
$n_l$	2	$\forall x \in [2500, 5000]$
$v_m$	4	$\forall x \in [2500, 5000]$

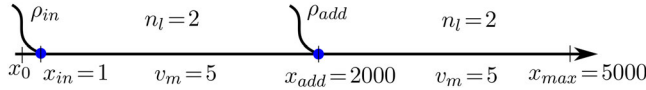


**Figure 12.** Schematic of merging roads.

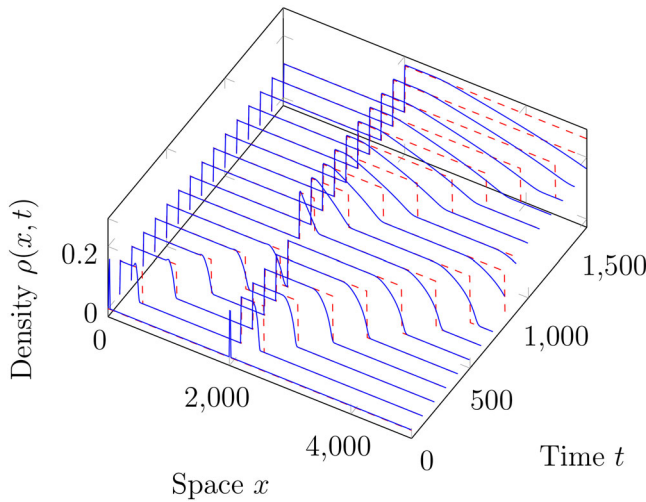


**Figure 13.** Modeling of road merging in free-flow traffic conditions: simulation with LBM in solid blue and with triangular-Daganzo fundamental diagram for LWR method in dashed red.

#### 4.4. Road merging

Changes of the traffic conditions can be caused by road merging. To study the effects of road merging on traffic conditions, the simulation of a two-lane highway is considered. It can be remarked that the interaction of road merging is acting both ways: if the sum of the two density exceeds the critical density of the highway, then congested situations can propagate backward in both roads. Thus, we propose the following expression of the interaction at the merging point:

$$\rho(x_{add}) = \begin{cases} \rho(x_{add}-1) + \rho_{add} & \text{if } \rho(x-1) + \rho_{add} \leq \rho_{critic} \\ \rho(x_{add}) + 0.3\rho_{add} & \text{else} \end{cases} \quad (31)$$

This road is constituted of 5000 cells and the speed limit is 5 cells per unit of time. The complete highway is empty at the time  $t = 0$  of the

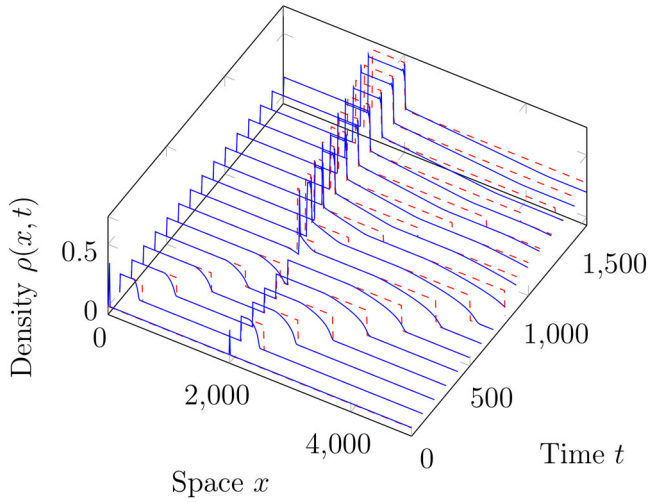


**Figure 14.** Modeling of road merging in congested-flow traffic conditions: simulation with LBM in solid blue and with triangular-Daganzo fundamental diagram for LWR method in dashed red.

**Table 5.** Parameters for the LBM modeling of road merging in free-flow traffic conditions.

Parameters	Values	Space
$\rho_{in}$	0.11	$x_{in} = 1$
$n_l$	2	$\forall x \in [0, 2000]$
$v_m$	5	$\forall x \in [0, 2000]$
$\rho_{add}$	0.15	$x_{add} = 200$
$n_l$	2	$\forall x \in [2000, 5000]$
$v_m$	5	$\forall x \in [2000, 5000]$

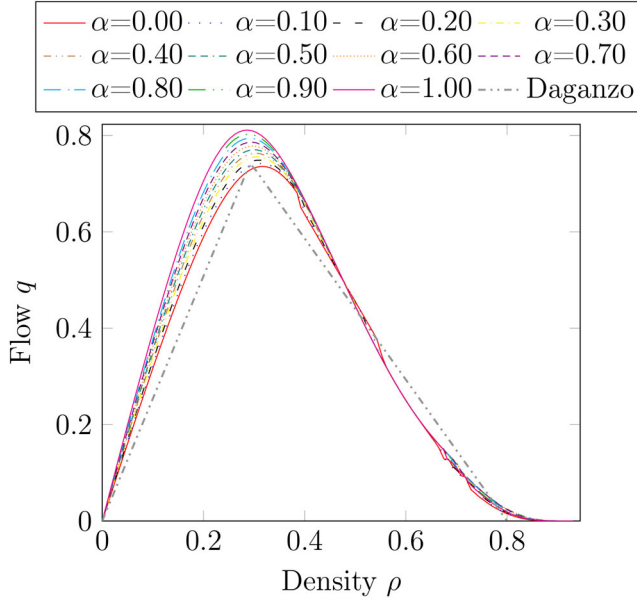
simulation. At the beginning of the road, the density is set to a constant, while 2000 cells further a road merging adds another constant density except if the sum is higher than one (see Figure 12).

Figure 13 illustrates the dynamic of the density when the two flows merge. The density at the edge of the simulation is set to 0.11 and the incident density is set to 0.15 (see Table 5). These two density and their sum are in free-flow conditions: when the flows joined the density is simply the sum of the incoming density. Therefore, no jam is observed around the merge.

*Per contra*, Figure 14 is obtained with an initial density of 0.15 at the beginning of the road and an incident density of 0.20 (see Table 6). These two ones are still in free-flow domain but not their sum. Therefore, as expected, Figure 14 shows a slowing down waves (characterized by an increase of the density) streaming backward from the merging point.

**Table 6.** Parameters for the LBM modeling of road merging in congested-flow traffic conditions.

Parameters	Values	Space
$\rho_{in}$	0.15	$x_{in} = 1$
$n_l$	2	$\forall x \in [0, 2000]$
$v_m$	5	$\forall x \in [0, 2000]$
$\rho_{add}$	0.20	$x_{add} = 200$
$n_l$	2	$\forall x \in [2000, 5000]$
$v_m$	5	$\forall x \in [2000, 5000]$



**Figure 15.** Fundamental diagram: flow-density relationship for different lorry concentration.

#### 4.5. Truck concentration

To evaluate the effects of heterogeneous multi-class traffic, a ring road is studied. The simulation of section 4.1 is reused but a variable ratio of 2 vehicle classes is put in the model. These two classes have different speed limits: one has a speed limit of 5 cells per unit of time, while the other has a speed limit of only 4. The ring road is made of 1000 cells, 3 lanes (see Figure 3). The injection point imposes a global density  $\rho_p$  distributed in two classes, through a coefficient  $\alpha$ . Thus,  $\rho_1(x_p) = \alpha\rho_p$  and  $\rho_2(x_p) = (1-\alpha)\rho_p$ .

Figure 15 shows the influence of a class of slower vehicles (with index 2), with a speed limit of 4 cells per unit of time (to simulate the heavy weighted machines), on a class of faster ones (with index 1) having a speed limit of 5 cells per unit of time (to model the personal cars).

Figure 15 shows the fundamental diagrams obtained.

It highlights that the maximum possible flow is lower with slower vehicles. This is even more drastic when putting back the right problem

dimensions in the fundamental diagram. Indeed, if the slower vehicles are lorries, they are more represented through the Equation (12), since they have longer length.

## 5. Discussions & perspectives

The suggested method allows to reproduce macroscopic situations from a mesoscopic formulation through a Boltzmann-like equation. The present lattice-Boltzmann method is capable of modeling the theoretical traffic behavior described in the literature. In particular, the results obtained with the present model is able to recover those of Drake's model. However, the suggested method also adds the possibility to include the basic psychological behavior of drivers through the relaxation time parameter. This also implies at least two elements of improvement. The first is the adaptive setting of the relaxation time to weather conditions or physiological parameters such as the tiredness (before holiday periods or after long/difficult travels). The second is a work around the collision operator that could gather the inclusion of psychological behavior and numerical efficiency.

Thanks to the improved formulation, the simulation of various road situations, unprecedented with such method, is now allowed. Conventional microscopic or macroscopic methods are able to furnish simulations of many road situations, but the previous works using the LBM never demonstrated their ability to capture these situations. Through our incorporation of the number of lanes in the Equations (16), (29), and (30), it is possible to obtain simulations of roads with a number of lanes changing in free flow domain and respectively in congested domain shown on Figure 7 and respectively on Figure 8. Moreover, as it is suggested with the introduction of the speed limit parameter in the Equations (27) and (28), it allows to simulate roads with a variable speed limit both in free flow and congested domain. These situations of roads with a variable speed limit are represented on Figure 7 and on Figure 8. In all the situations studied: number of lanes, speed restriction change and road merging, the LBM gives dynamic results very closes to those from LWR method, while providing mesoscopic information details.

The merging roads, which implies a new mesoscopic implementation of the boundary conditions for the numerical simulations. This contribution about the boundary conditions is necessary to simulate realistic configurations. Furthermore, thanks to the mesoscopic nature of the LBM the roads merging with an active traffic light system is also imaginable (Gartner and Wagner 2004; Newell 1956). Of course, new improvements are imaginable, to extend the number of realistic situations reachable by the method. Diverging roads branch simulation could be very useful, particularly with

the possibility to connect LBM simulations of different roads. Then, it would be possible to simulate a large highway network from the traffic input and output measures and compare it to real observations to improve the methods and models.

To obtain more realistic traffic situations, the influence of heavy machine is of first importance and has many impacts. To incorporate several vehicle classes, the constitutive equations of the LBM are adapted. This adaptation is performed through the [Equations \(24\)–\(30\)](#). Therefore, all the previous situations with changes of road properties can be simulated with a mixture of vehicle classes. To emphasize only the effect of multi-class mixture, the study of a ring road is preferred and given on [Figure 15](#). The influence of a multi-class traffic, on fundamental diagram, found here is close to those presented by some authors Ez-Zahraouy, Jetto, and Benyoussef (2004). Nevertheless, since the very simple assumption of symmetrical interaction with all the vehicles regardless of their class is made, a logical improvement could be included the psychological aspects of drivers facing trucks or smaller cars. These improvements imply to treat nonsymmetrical class interactions and could have connections with non-miscible fluids mixture well addressed by the LBM.

Other aspects such as the sinuosity of the road or the traffic pressure in multi-class flows could be interesting to add to the model. Moreover, the mesoscopic scale and the statistical nature of the LBM could be turned into a greater advantage by bringing at that scale stochastic variation of the distribution function to represent realistic random events. Investigations on the equilibrium distribution functions and their justification would also be an important step. The frequency with which the virtual boundary condition is used could also be linked with the probability of real car accident, since this boundary implies a quick breaking action in order to avoid exceeding the road capacity.

Thus, the suggested method is able to deal with road merging, change of lane numbers or speed limits with multi-class vehicles effects in both free-flow and congested-flow conditions in agreement with the macroscopic previsions. Even if these capacities of simulations are new with the LBM, these are very common with standard methods. However, the LBM presents many interesting aspects not present in standard methods. Indeed, the LBM is yielding mesoscopic solutions with a reduced computational time, and its local and explicit nature make it highly parallelizable. Plus, statistical aspects of the method could be useful for stochastic parameters and simulations Wagner, Buisson, and Nippold (2016). Therefore, the presented extension and validation of traffic flow simulations with the LBM is a step before many further possible developments.

## 6. Conclusions

The lattice Boltzmann method is an efficient numerical method to overcome the integro-differential difficulties introduced by statistical models and might be a practical manner to solve numerically the Prigogine-Boltzmann like equation. This remains a good compromise between, on the one hand, the high level of detail (but time consuming provided by the microscopic description) and, on the other hand, the loss of information (but the faster computation yield by the macroscopic description). Moreover, the macroscopic results obtained through the LBM are bounded to the choice of the equilibrium density function that can be tuned to reproduce various effects and models.

The presented results demonstrate the capacity of the LBM to solve heterogeneous multi-class traffic flows, and suggested formulations give easy treatment to deal with numerous road situations.

Indeed, thanks to this equilibrium density function and some extensions done by introducing parameters like the number of lanes and the speed limit or some boundary conditions, the ability for the suggested method to reproduce situations such as roads merging, changing the number of lanes or changing the speed limits in all traffic domains (free-flows or congested-flows) is also demonstrated.

In addition, the complete adaptation of all the equations to incorporate the mixture of heterogeneous multi-class is performed. This adaptation permits to simulate and validate the effect of lorries mixes with faster cars in case of miscible phases.

Thus, the presented article investigated the use of the LBM for traffic flow simulations. Beyond this method which is scarcely used for these problems, the method is here extended to reach more realistic simulations. This work of validation is necessary before exploring the numerous development opened by this numerical mesoscopic method.

## Acknowledgment

The authors would like to thank Solenn Bardaud and Elias Abou Rachid for their participation in numerical implementations.

## Conflict of interest

The authors declare no potential conflict of interest of any kind.

## Funding

This work has been partially funded by the French National Research Agency via the LBSMI project ANR-15-CE19-0002.

## ORCID

Romain Noël  <http://orcid.org/0000-0003-4322-6125>

Laurent Navarro  <http://orcid.org/0000-0002-8788-8027>

Guy Courbebaisse  <http://orcid.org/0000-0001-6181-2000>

## References

- Bagnerini, P., and M. Rascle. 2003. A multiclass homogenized hyperbolic model of traffic flow. *SIAM J. Math. Anal.* 35 (4):949–73.
- Bhatnagar, P. L., E. P. Gross, and M. Krook. 1954. A model for collision processes in gases. I. Small amplitude processes in charged and neutral one-component systems. *Phys. Rev.* 94 (3):511–25.
- Cercignani, C. 1988. *The Boltzmann equation and its applications. Vol. 67 of Applied mathematical sciences.* New York, NY: Springer New York.
- Chanut, S. 2005. Modélisation dynamique macroscopique de l'écoulement d'un trafic routier hétérogène poids lourds et véhicules légers. PhD thes., Institut National des Sciences Appliquées de Lyon.
- Chen, C., L. Li, J. Hu, and C. Geng. 2010. Calibration of MITSIM and IDM car-following model based on NGSIM trajectory datasets. In Proceedings of 2010 IEEE International Conference on Vehicular Electronics and Safety, QingDao, China, Jul., 48–53.
- Chopard, B., A. Dupuis, A. Masselot, and P. Luthi. 2002. Cellular automata and lattice Boltzmann techniques: An approach to model and simulate complex systems. *Adv. Complex Syst.* 05 (02n03):103–246.
- Chopard, B., P. O. Luthi, and P.-A. Queloze. 1996. Cellular automata model of car traffic in a two-dimensional street network. *J. Phys. A: Math. Gen.* 29 (10):2325–36.
- Costeseque, G., and A. Duret. 2015. Mesoscopic multiclass traffic flow modeling on multi-lane sections. The 95th Transportation Research Board (TRB) Annual Meeting, Washington, DC, 28.
- Daganzo, C. F. 1997. A continuum theory of traffic dynamics for freeways with special lanes. *Transp. Res. Part B: Methodol.* 31 (2):83–102.
- Delis, A. I., I. K. Nikolos, and M. Papageorgiou. 2018. A macroscopic multi-lane traffic flow model for ACC/CACC traffic dynamics. *Transp. Res. Rec.* 2672 (20):178–92.
- Drake, J. S., J. L. Schofer, and A. D. May, Jr. 1967. A statistical analysis of speed density hypotheses. *Charact. Traffic Flow* 45:53–87.
- Ez-Zahraouy, H., K. Jetto, and A. Benyoussef. 2004. The effect of mixture lengths of vehicles on the traffic flow behaviour in one-dimensional cellular automaton. *Eur. Phys. J. B* 40 (1):111–7.
- Gartner, N. H., and P. Wagner. 2004. Analysis of traffic flow characteristics on signalized arterials. *Transp. Res. Rec.* 1883 (1):94–100.
- Gazis, D. C., R. Herman, and R. W. Rothery. 1961. nonlinear follow-the-leader models of traffic flow. *Oper. Res.* 9 (4):545–67.
- Gipps, P. G. 1981. A behavioural car-following model for computer simulation. *Transp. Res. Part B: Methodol.* 15 (2):105–11.
- Greenberg, H. 1959. An analysis of traffic flow. *Oper. Res.* 7 (1):79–85.
- Greenshields, B. D. 1935. A study of traffic capacity. In Highway Research Board Proceedings, Vol. 14 of Proceedings of Annual Meeting, Washington, DC, Dec., 448–77. Highway Research Board.



- He, X., and L.-S. Luo. 1997. Theory of the lattice Boltzmann method: From the Boltzmann equation to the lattice Boltzmann equation. *Phys. Rev. E* 56 (6):6811–7.
- Helbing, D. 2001. Traffic and related self-driven many-particle systems. *Rev. Mod. Phys.* 73 (4):1067–141.
- Helbing, D., A. Hennecke, V. Shvetsov, and M. Treiber. 2002. Micro- and macro-simulation of freeway traffic. *Math. Comput. Modell.* 35 (5-6):517–47.
- Hidas, P. 2002. Modelling lane changing and merging in microscopic traffic simulation. *Transp. Res. Part C: Emerg. Technol.* 10 (5-6):351–71.
- Holme, R., and D. H. Rothman. 1992. Lattice-gas and lattice-Boltzmann models of miscible fluids. *J. Stat. Phys.* 68 (3-4):409–29.
- Hoogendoorn, S. P., and P. H. L. Bovy. 2000. Continuum modeling of multiclass traffic flow. *Transp. Res. Part B: Methodol.* 34 (2):123–46.
- Hoogendoorn, S. P., and P. H. L. Bovy. 2001. Platoon-based multiclass modeling of multi-lane traffic flow. *Netw. Spat. Econ.* 1 (1/2):137–66. doi:[10.1023/A:1011533228599](https://doi.org/10.1023/A:1011533228599)
- Inamuro, T., M. Yoshino, H. Inoue, R. Mizuno, and F. Ogino. 2002. A lattice Boltzmann method for a binary miscible fluid mixture and its application to a heat-transfer problem. *Comput. Phys.* 179 (1):201–15.
- Jiang, R., and Q.-S. Wu. 2004. Extended speed gradient model for mixed traffic. *Transp. Res. Rec.* 1883 (1):78–84.
- Kerner, B. 1999. Congested traffic flow: Observations and theory. *Transp. Res. Rec.* 1678 (1):160–7.
- Kerner, B. S., S. L. Klenov, and D. E. Wolf. 2002. Cellular automata approach to three-phase traffic theory. *J. Phys. A: Math. Gen.* 35 (47):9971–10013.
- Kesting, A., M. Treiber, and D. Helbing. 2010. Enhanced intelligent driver model to access the impact of driving strategies on traffic capacity. *Philos. Trans. A Math. Phys. Eng. Sci.* 368 (1928):4585–605. doi:[10.1098/rsta.2010.0084](https://doi.org/10.1098/rsta.2010.0084)
- Lan, L. W., and C.-W. Chang. 2005. Inhomogeneous cellular automata modeling for mixed traffic with cars and motorcycles. *ATR* 39 (3):323–49.
- Lighthill, M. J., and G. B. Whitham. 1955. On kinematic waves. II. A theory of traffic flow on long crowded roads. *Proc. R. Soc. A: Math. Phys. Eng. Sci.* 229 (1178):317–45.
- Logghe, S., and L. H. Immers. 2008. Multi-class kinematic wave theory of traffic flow. *Transp. Res. Part B: Methodol.* 42 (6):523–41.
- Meng, J., Y. Qian, X. Li, and S. Dai. 2008. Lattice Boltzmann model for traffic flow. *Phys. Rev. E Stat. Nonlin. Soft. Matter Phys.* 77 (3 Pt 2):036108. doi:[10.1103/PhysRevE.77.036108](https://doi.org/10.1103/PhysRevE.77.036108)
- Munjal, P. K., and J. Pahl. 1969. An analysis of the Boltzmann-type statistical models for multi-lane traffic flow. *Transp. Res.* 3 (1):151–63. doi:[10.1016/0041-1647\(69\)90112-9](https://doi.org/10.1016/0041-1647(69)90112-9)
- Nagel, K., and M. Schreckenberg. 1992. A cellular automaton model for freeway traffic. *J. Phys. I France* 2 (12):2221–9.
- Nagel, K., D. E. Wolf, P. Wagner, and P. Simon. 1998. Two-lane traffic rules for cellular automata: A systematic approach. *Phys. Rev. E* 58 (2):1425–37.
- Newell, G. F. 1956. Statistical analysis of the flow of highway traffic through a signalized intersection. *Quart. Appl. Math.* 13 (4):353–69.
- Newell, G. F. 1993. A simplified theory of kinematic waves in highway traffic, Part II: Queueing at freeway bottlenecks. *Transp. Res. Part B: Methodol.* 27 (4):289–303.
- Newell, G. F. 2002. A simplified car-following theory: A lower order model. *Transp. Res. Part B: Methodol.* 36 (3):195–205.
- Ngoduy, D. 2011. Multiclass first-order traffic model using stochastic fundamental diagrams. *Transportmetrica* 7 (2):111–25.

- Paveri-Fontana, S. L. 1975. On Boltzmann-like treatments for traffic flow: A critical review of the basic model and an alternative proposal for dilute traffic analysis. *Transp. Res.* 9 (4):225–35.
- Payne, H. J. 1971. Models of freeway traffic and control. In *Mathematical Models of Public Systems: Simulation Council Proceedings*, Vol. 28, La Jolla, CA, 51–61. Simulation Councils Incorporation.
- Peeta, S., P. Zhang, and W. Zhou. 2005. Behavior-based analysis of freeway car–truck interactions and related mitigation strategies. *Transp. Res. Part B: Methodol.* 39 (5):417–51.
- Pipes, L. A. 1967. Car following models and the fundamental diagram of road traffic. *Transp. Res.* 1 (1):21–9.
- Pourabdollah, M., E. Bjarkvik, F. Furer, B. Lindenberg, and K. Burgdorf. 2017. Calibration and evaluation of car following models using real-world driving data. In *2017 IEEE 20th International Conference on Intelligent Transportation Systems (ITSC)*, Yokohama, Oct., 1–6. IEEE. doi:[10.1109/ITSC.2017.8317836](https://doi.org/10.1109/ITSC.2017.8317836)
- Prigogine, I., and F. C. Andrews. 1960. A Boltzmann-like approach for traffic flow. *Oper. Res.* 8 (6):789–97.
- Prigogine, I., and R. C. Herman. 1971. *Kinetic theory of vehicular traffic*. 1st ed. New York: American Elsevier Pub. Co.
- Richards, P. I. 1956. Shock waves on the highway. *Oper. Res.* 4 (1):42–51.
- Schadschneider, A., and M. Schreckenberg. 1993. Cellular automation models and traffic flow. *J. Phys. A: Math. Gen.* 26 (15):L679–L683.
- Shan, X., and H. Chen. 1993. Lattice Boltzmann model for simulating flows with multiple phases and components. *Phys. Rev. E Stat. Phys. Plasmas. Fluids. Relat. Interdiscip. Topics* 47 (3):1815–9. doi:[10.1103/physreve.47.1815](https://doi.org/10.1103/physreve.47.1815)
- Shi, W., W.-Z. Lu, Y. Xue, and H.-D. He. 2016. Revised lattice Boltzmann model for traffic flow with equilibrium traffic pressure. *Phys. A.* 443:22–31.
- Shvetsov, V., and D. Helbing. 1999. Macroscopic dynamics of multilane traffic. *Phys. Rev. E Stat. Phys. Plasmas. Fluids. Relat. Interdiscip. Topics* 59 (6):6328–39. doi:[10.1103/physreve.59.6328](https://doi.org/10.1103/physreve.59.6328)
- Succi, S. 2001. *The lattice Boltzmann equation for fluid dynamics and beyond. Numerical mathematics and scientific computation*. Oxford: Clarendon Press; Oxford University Press.
- Talebpoor, A., and H. S. Mahmassani. 2016. Influence of connected and autonomous vehicles on traffic flow stability and throughput. *Transp. Res. Part C: Emerg. Technol.* 71:143–63.
- Treiber, M., and A. Kesting. 2013. *Traffic flow dynamics*. Berlin: Springer Berlin Heidelberg.
- Wagner, P., C. Buisson, and R. Nippold. 2016. Challenges in applying calibration methods to stochastic traffic models. *Transp. Res. Rec.* 2560 (1):10–6.
- Wolf-Gladrow, D. A. 2000. *Lattice-gas cellular automata and lattice Boltzmann models: An introduction. Lecture notes in mathematics*. Vol. 1725. New York: Springer.
- Wu, C., A. Kreidieh, E. Vinitsky, and A. M. Bayen. 2017. Emergent behaviors in mixed-autonomy traffic. In *Conference on Robot Learning*, Mountain View, CA, USA, Oct., 398–407.